

Effect of liquid density on particulate flow in dam break

Gyeong Min Park¹, Hyun Sik Yoon^{2*}, Min Il Kim¹

¹School of Mechanical Engineering, Pusan National University, Busandaehak-ro 63beon-gil, Geumjeong-gu, Busan 609-735, Korea.

²Global Core Research Center for Ships and Offshore Plants, Pusan National University, 2, Busandaehak-ro 63beon-gil, Geumjeong-gu, Busan 609-735, Korea.

*Corresponding author: lesmodel@pusan.ac.kr

Abstract: - The present study investigated the dam breaking containing the particles by handling three phases of the liquid-gas-solid mixture. The discrete element method (DEM) - computational fluid dynamics (CFD) combined method was adopted to resolve the three phases of the liquid-gas-solid mixture. The present study considers the wide range of the liquid density to investigate the effect of the liquid density on the behavior of the particles and the free-surface. Three regimes of the overlapping, divergent and impinging behaviors govern the time evolution of the particles and the free-surface. The overlapping regime shows that the front head positions of the liquid and the particles are almost identical and two dimensional behaviors. However, in the divergent regime, lower liquid densities derive that the liquid front head is faster than that of the particle. Over the critical liquid density, the opposite divergent pattern to the low liquid density appears. Especially, the three-dimensional effect on the distribution of the particles and the free-surface appears in the divergent regime.

Key-Words: - DEM, CFD, Three phases, Liquid-gas-solid mixture, Three regimes

1 Introduction

The liquid-gas-solid (particle) mixture is very important in wide areas of the academics, industries and also the real life. In addition, because of its natural complexity to be investigated by the numeric and experimental methods, the problem containing liquid-gas-solid mixture is greatly challenged by numerous researchers.

For examples, the failure of a natural dam can initiate a debris flow that are dangerous to life and property [1], which results in the catastrophic disaster and simultaneously the downstream flood damage. Also, in the safety analysis of core disruptive accidents of a liquid metal cooled reactor, sloshing dynamics of a molten core strongly affects the entire progression of an accident and correlated consequences. In addition, the movements and the interactions, for example, of refrozen fuels and disrupted pellets in the molten core are other concerns and sources of difficulties that significantly influence sloshing in molten core [2]. Therefore, the prediction of the liquid-gas-solid mixture flow is fundamental to prevent and minimize the risk.

The present study considers the particles containing dam break problem which can correspond to the typical liquid-gas-solid problem.

As an element of the present problem, the dam break has been intensively studied as one of the popular liquid-gas problems to identify an interaction of liquid-gas in various fields [3-12]. However, it is hard to find the researches relevant to the present study which covers the dam break flow containing a particle bed, based on the three phases of liquid-gas-solid.

A few studies have handled the single fluid-solid phase. Guo and Morita [2] investigated the sloshing in a liquid-solid mixture by using the finite volume particle (FVP)-DEM coupled method. Also, Sun et al. [3] studied various solid-liquid flows (dam break and rotating cylindrical tank) by using DEM-smoothed particle hydrodynamics (SPH).

Recently, Sun and Sakai [13] conducted experiment and CFD-DEM simulation for dam break problem containing particles. Thus, their problem is based on three phases of liquid-gas-solid. The main focus of their study is not to interpret the physics of three-phase problem but to validate the adopted numerical methods of CFD-DEM by comparing the simulation results with the experimental ones.

Based on authors' literature survey, as mentioned above, it is hard to find the not only numerical simulations but also experiments which dealt the three-phase based dam breaking problem. Especially,

there is no study which provides the physical interpretation for the various conditions in terms of the fluid and particle properties and water column.

Therefore, as the initial study for the three-phases of liquid-gas-solid based dam breaking problem, the present research aims at investigating the effect of the liquid density on the behaviors of the particles and the liquid under the circumstance of the dam breaking by using the CFD-DEM combined simulations.

2 Description of numerical simulation

The fluid motion is solved CFD based approach with gas-liquid interface capturing provided by the volume of fraction (VOF). The particle phase is tracked by DEM as discrete entities.

2.1 Governing equations of particle motion

The movement of a particle is described by DEM. Contact forces are described by the Voigt model which consists of spring, dash pot and slider. At time t , the translational displacement v_a of particle a with the mass of m_a by the contact force that acts between two particles is given in Eq. (1).

$$m_a \frac{dv_a}{dt} = F_n + F_g + F_{fluid} \quad (1)$$

The right hand side contains terms for the normal direction contact (F_n), gravity (F_g) and fluid forces (F_{fluid} consists of drag and pressure gradient forces). In Eq. (1), the normal direction contact forces are calculated using the linear spring contact model.

Besides translational motion, particles also undergo rotational motion which is governed by Eq. (2)

$$I_a \frac{d\omega_a}{dt} = T_a (= R_a \times F_t) \quad (2)$$

where I_a , ω_a , T_a , R_a , F_t and M_a are the moment of inertia, the angular velocity, the torque generated by the tangential forces, the distance from the center of mass to the contact point and the tangential direction contact force, respectively. Further details of the implementation can be found in Sun and Sakai [13].

2.2 Governing equations of fluids flow

The present three-dimensional two-phase flow is governed by the continuity equation in Eq. (3), the Navier–Stokes equation in Eq. (4).

$$\frac{\partial \varepsilon u_i}{\partial x_i} = 0 \quad (3)$$

$$\begin{aligned} \frac{\partial}{\partial t} (\rho \varepsilon u_i) + \frac{\partial}{\partial x_j} (\varepsilon \rho u_i u_j) = -\varepsilon \frac{\partial p}{\partial x_i} \\ + \frac{\partial}{\partial x_j} \left[\varepsilon \mu \left(\frac{\partial u_i}{\partial x_j} + \frac{\partial u_j}{\partial x_i} \right) \right] + \varepsilon \rho g - S_m \end{aligned} \quad (4)$$

where x_i is Cartesian coordinates, u_i is the corresponding velocity components, p is the pressure, ρ is the density, μ is the viscosity, ε is the porosity and g is the gravity. The source term S_m take into account the interaction force between fluid and particles by two-way coupling.

In this study, the VOF method is employed to capture the free surface of two-phase flow. In each cell, the volume fraction (Q_δ) of the δ th fluid is introduced because this method is designed for two or more immiscible fluids.

$$\varepsilon \frac{\partial Q_\delta}{\partial t} + \varepsilon u_i \frac{\partial Q_\delta}{\partial x_i} = 0 \quad (5)$$

Convection and diffusion terms are discretized using the second order upwind scheme and the second order central differencing scheme, respectively. For unsteady flow calculations, time derivative terms are discretized using the second order accurate backward implicit scheme. The velocity–pressure coupling and overall solution procedure are based on a SIMPLE-type segregated algorithm adapted to an unstructured grid.

2.3 Computational domain specification

The computational domain is shown in Fig. 1 where the dimensions of the length, breadth and height are 0.2, 0.1 and 0.3 (m), respectively.

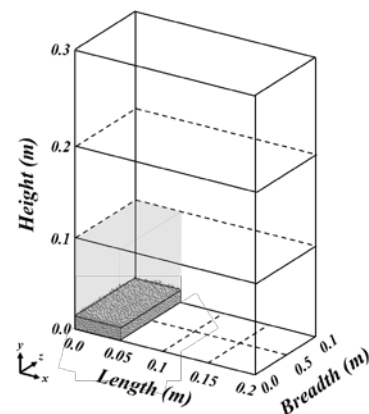


Fig. 1 The schematic of the computational domain.

Fig.2 illustrates typical two dimensional dam breaking flow with particle bed. The reservoir's initial length (L_R), breadth and height (H_R) are 0.05,

0.1 and 0.1 (m) respectively. The rest of the computational domain is assumed to be air.

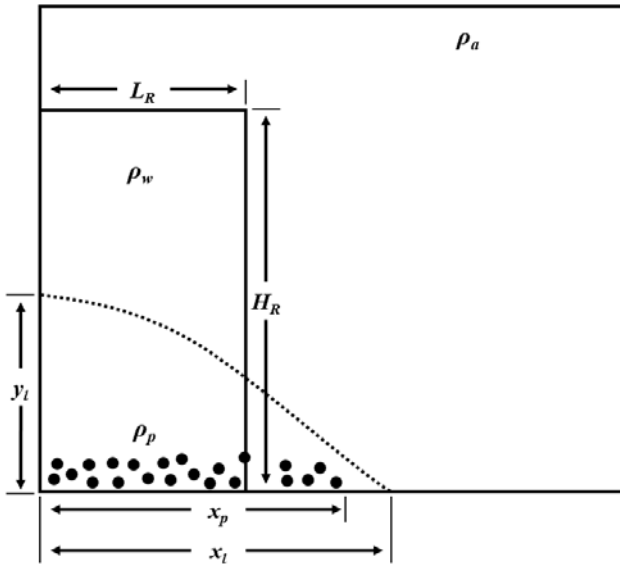


Fig. 2 The dam break flow with particle bed

The dimensionless variables used in this study are time (t^*), liquid front head position (x_l^*), liquid height (y_l^*), particle front head position (x_p^*). They are described as follows:

$$t^* = t(2g/L_R)^{1/2} \quad (6)$$

$$x_l^* = x_l / L_R \quad (7)$$

$$y_l^* = y_l / L_R \quad (8)$$

$$x_p^* = x_p / L_R \quad (9)$$

No-slip boundary condition is imposed on the vertical and horizontal walls.

Tables 1 and 2 show the properties of particle and fluids, respectively.

Table 1 Parameter of particle

Type	Glass beads
Diameter (m)	0.0027
Density, ρ_p (kg/m^3)	2,500
The number of particles	3,883
Total mass of particles (g)	100
Spring constant (N/m)	1,000
Restitution coefficient	0.9
Friction coefficient	0.3

Table 2 Properties of fluids

Liquid density, ρ_l (kg/m^3)	1000, 1500, 2000, 2400
Liquid viscosity (Pa·s)	10^{-3}
Air density, ρ_a (kg/m^3)	1

Air viscosity (Pa·s)	10^{-5}
----------------------	-----------

2.4 Validation

To assure the validity of numerical methods, the quantitative comparison between the present results and Sun and Sakai [13]'s ones is carried out for the time histories of normalized positions of the liquid front head. Fig. 3 shows the favorable comparison with Sun and Sakai [13]'s results.

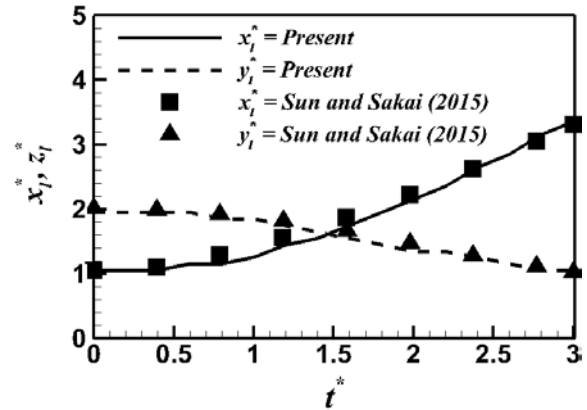
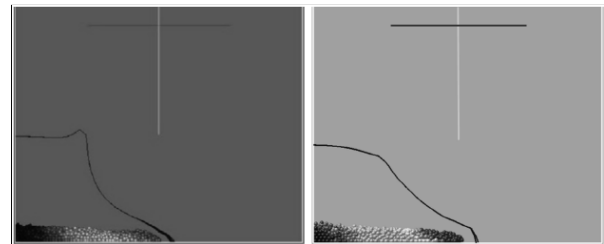
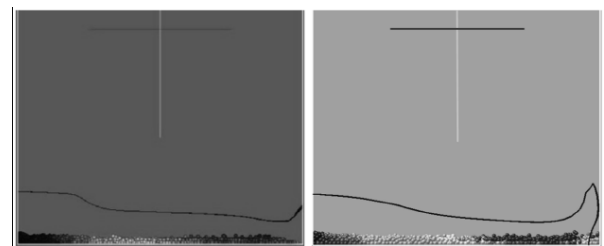


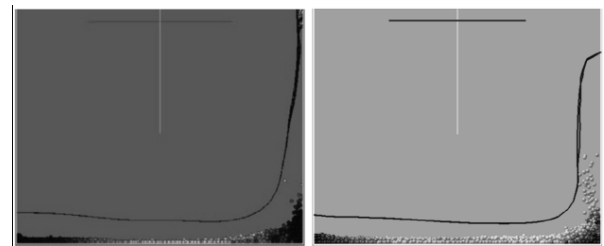
Fig. 3 Comparison of normalized position with the present results (solid line) and Sun and Sakai [13]'s ones (square symbol).



(a)



(b)



(c)

Fig. 4 Comparison of particles distribution and free-surface formation at (a) $t=0.1$ s, (b) $t=0.2$ s and (c)

$t=0.3$ s with the present results (right column) and Sun and Sakai [4]'s results (left column).

Figure 4 shows the comparison of the present particles distribution and free-surface formation in the time sequence of dam break flow with Sun and Sakai [4]'s results. Particles' motion is captured by scattered dots with their velocity contours. The present and Sun and Sakai [13] represents the identical results as follows. The moving particle bed that moves more slowly than the water front head does in early stages of the dam break for $t < 0.2$ s. And then, the solid particle bed expands over the floor of the tank and the water hits the vertical wall. The bulk of the water-particle mixture goes on moving forward and strongly impacts against the tank, which leads to a high water jet attached to the wall at $t = 0.3$ s. The solid layer also follows this motion, as it is found that at the left corner of the tank lies a pile of particles as well as some splashing ones.

As a result of the above excellent comparison, the present numerical methods are reliable to handle three phase flow problem.

3 Result and discussion

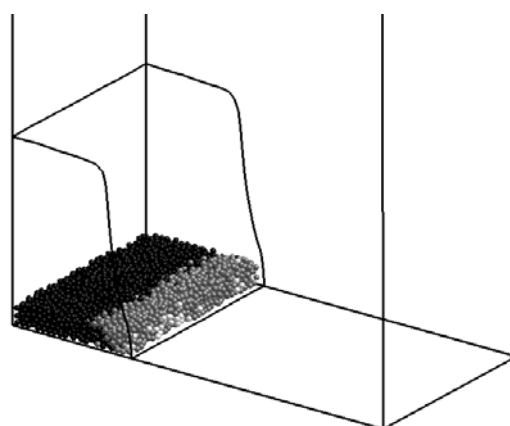
Figure 5 presents the typical three dimensional perspective views which show the time evolution of the particles and the free-surface between the liquid and the gas for $\rho_l = 1000 \text{ kg/m}^3$. When the liquid starts to collapse by the gravity, the front head of the liquid and the particles becomes advance against the wall. At the initial stage of the dam breaking, the front head positions of the liquid and the particles are almost identical, as shown in Fig. 5(a). This stage is designated as the overlapping regime of the front head positions of the liquid and the particles.

As time goes by, the liquid front head becomes faster than that of the particles, as shown in Fig. 5(b). Thus, this stage is named as the divergent regime. Successively, the liquid early impinges on the wall and then goes up due to the inertia, which can be identified Fig. 5(c). Finally, the impinging regime covers the classification of the time evolution of the particles and the free-surface. The time period of each regime is dependent on the liquid density, which will be dealt later.

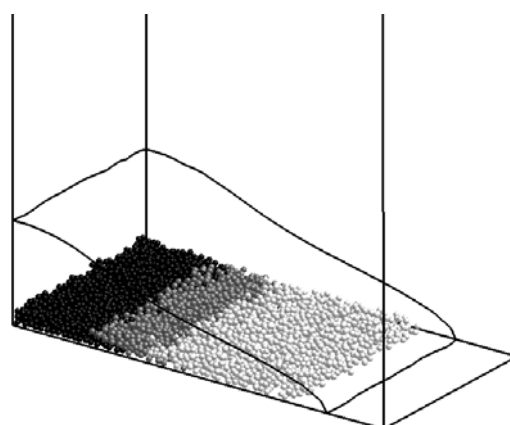
The front head positions of the liquid for different liquid densities are plotted in Fig. 6. In general, the front head positions for different liquid densities have about the same profile which is governed by the parabolic pattern. Therefore, the initial variation of the front head position is almost negligible, resulting in very small advance velocity. Then, the front head position increases quickly. Therefore, the

front head speed becomes fast. Finally, near the wall before the impinging regime, the front head speed decelerates. This variation of the front head speed according to liquid advance can be identified by the front head speed in Fig. 6.

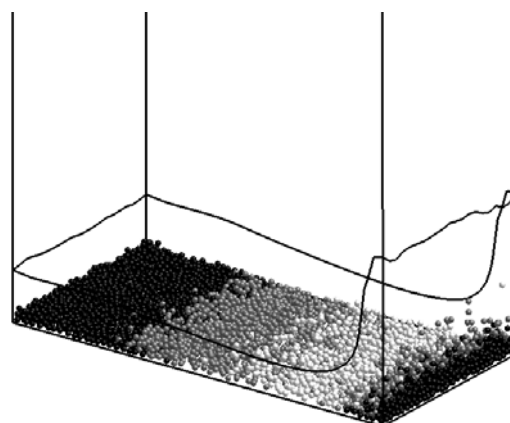
The dependence of the liquid front head position on the liquid density can be also clarified in Fig. 6. Generally, as the liquid density becomes larger, the liquid front head position increases.



(a)



(b)



(c)

Fig. 5 Snapshots of the particulate flow in dam break for water density of 1000 kg/m^3 at $t^*=1$, (b) $t^*=3$ and (c) $t^*=6$.

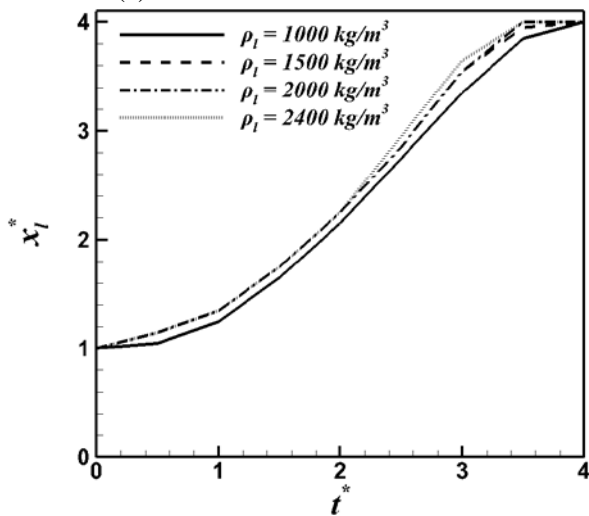


Fig. 6 Time histories of dimensionless position of liquid front head according to liquid density.

Figure 7 shows the front head positions of the particles for different liquid densities.

Regardless of the liquid density, the profile of the front head position of the particle is composed of three sections governed by the linear behaviour. The first regime has the smallest slope which corresponds to the front head speed. In this regime, the front head position is independent of the liquid density.

The second regime exposes the sharp slope which is induced by higher speed than the first regime. In this regime, the front head position depends on the liquid density. Resultantly, as the liquid density increases, the front head position of the particle increases. This suggests that the front head speed increases with increasing the liquid density. Finally, near the wall before the impinging regime, the front head position changes very slowly.

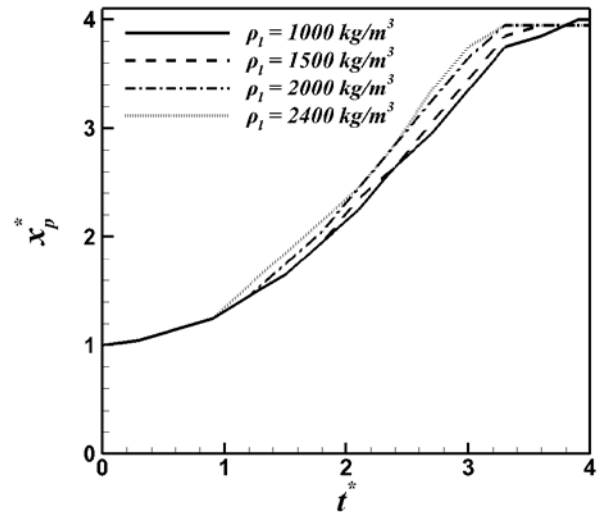


Fig. 7 Time histories of dimensionless position of particle front head according to the liquid density.

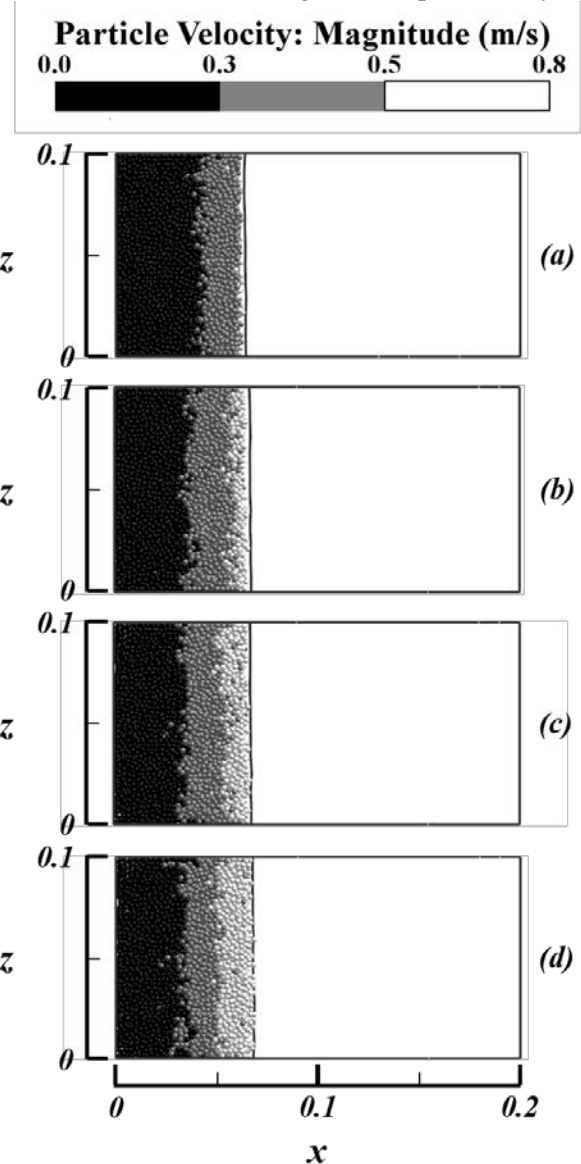


Fig. 8 Snapshots of the particulate flow in dam break for water density with different values of (a)

1000, (b) 1500, (c) 2000 and (d) 2400 at $t^* = 1$. Unit of density: kg/m^3 .

Figure 8 shows the top views of particles and the free-surface for different liquid densities. As early discussed in Fig. 4 showing the typical three dimensional perspective views of particles and the free-surface, the time evolution of the particles and the free-surface is classified by three regimes. Figure 8 represents the identical regime where the front head positions of the liquid and the particles are almost same. However, the overlapping location sustains longer distance with increasing the density. In this regime, the three dimensional effect is minor.

Regarding to the divergent regime, the typical distribution of particles and the free-surface for different liquid densities is plotted in Fig. 9. In this regime, two divergent patterns appear according to the liquid density. First, the liquid front head is faster than that of the particle in the small density region, as shown in Fig. 9(a). Another pattern is opposite to first one, as shown in Figs. 9(c) and (d). It is noted that the co-existence regime of the divergent-overlapping pattern is observed at a critical density over which the regime is divergent, as shown in Fig. 9(c).

In contrast to the overlapping regime, the divergent regime shows the three dimensional effect in the spanwise and also the streamwise directions, because the instability is augmented by the increase of the velocity of the fluids and particles.

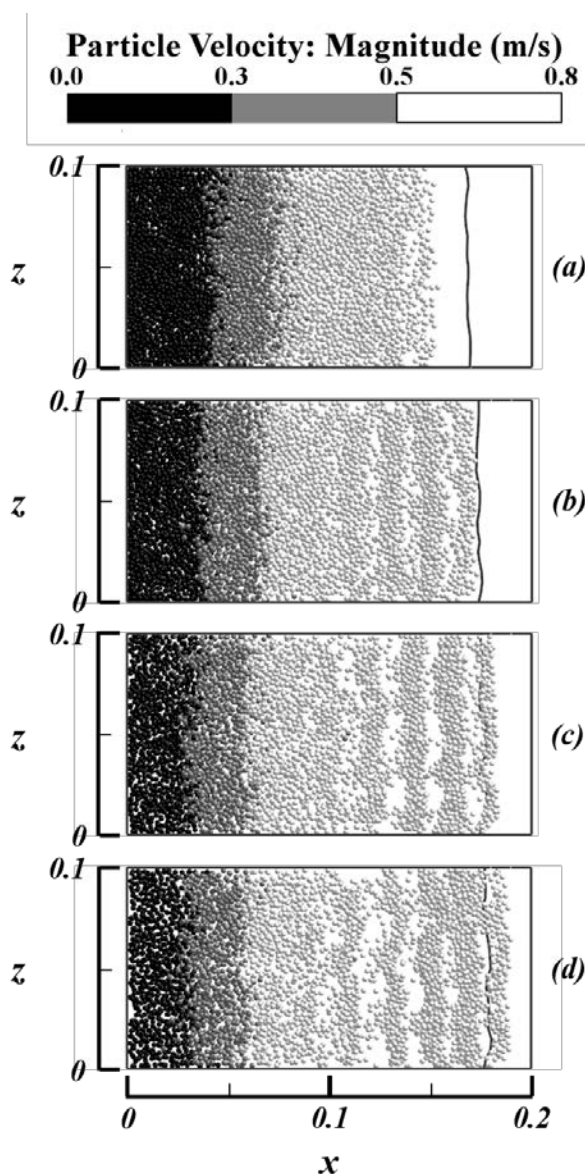


Fig. 9 Snapshots of the particulate flow in dam break for water density with the different values of (a) 1000, (b) 1500, (c) 2000 and (d) 2400 (kg/m^3) at $t^* = 3$. Unit of density: kg/m^3 .

4 Conclusion

The present study investigated the dam breaking containing the particles by handling the three phases of the liquid-gas-solid mixture. The DEM-CFD combined method was adopted to resolve the three phases of the liquid-gas-solid mixture. The present method was excellently validated by comparing the previous results obtained by the numerical and experimental methods to investigate the similar relevant problem to the present study. The main purpose of the present study is to investigate the effect of the liquid density on the behavior of the particles and the free-surface.

The time evolution of the particles and the free-surface is classified by three regimes of the overlapping, divergent and impinging behaviors. At the initial stage of the liquid collapse, the overlapping regime governs the front head positions of the liquid and the particles, resulting in that the front head positions of the liquid and the particles are almost identical.

The divergent regime contains two patterns. One is that the liquid front head is faster than that of the particle in the small density region. Another pattern is opposite to first one.

Acknowledgment

This work was supported by National Research Foundation of Korea (NRF) grant founded by the Korea government (MSIP) through GCRC-SOP (No. 2011-0030013).

References:

- [1] Highland, L., Ellen, S.D., Christian, S.B. and Brown, W.M., *Debris-Flow Hazards in the United States*, U.S. Department of the Interior, U.S. Geological Survey: Denver, CO, USA, 1997.
- [2] Guo, L. and Morita, K., Numerical simulation of 3D sloshing in a liquid–solid mixture using particle methods, *International Journal of Numerical Methods Engineering*, Vol.95, 2013, pp. 771–790.
- [3] Abdolmaleki, K., Thiagarajan, K. P., and Morris-Thomas, M. T., Simulation of the dam break problem and impact flows using a Navier-Stokes solver, *Australasian Fluid Mechanics Conference, 2004*
- [4] Shigematsu, T., Liu, P. L. F., and Oda, K., Numerical modeling of the initial stages of dam-break waves, *Journal of Hydraulic Research*, Vol.42, No.2, 2004, pp. 183-195.
- [5] Lobovský, L., Botia-Vera, E., Castellana, F., Mas-Soler, J., and Souto-Iglesias, A., Experimental investigation of dynamic pressure loads during dam break, *Journal of Fluids and Structures*, Vol. 48, 2014, pp. 407-434.
- [6] Hirt, C. W., and Nichols, B. D., Volume of fluid (VOF) method for the dynamics of free boundaries, *Journal of computational physics*, Vol.39, No.1, 1981, pp. 201-225.
- [7] Harlow, F. H., and Welch, J. E., Numerical calculation of time-dependent viscous incompressible flow of fluid with free surface, *Physics of fluids*, Vol.8, No.12, 1965, pp. 2182-2189.
- [8] Koshizuka, S., and Oka, Y., Moving-particle semi-implicit method for fragmentation of incompressible fluid, *Nuclear science and engineering*, Vol.123, No.3, 1996, pp. 421-434.
- [9] Colagrossi, A., and Landrini, M., Numerical simulation of interfacial flows by smoothed particle hydrodynamics, *Journal of Computational Physics*, Vo.191, No.2, 2003, pp. 448-475.
- [10] Shao, S., and Lo, E. Y., Incompressible SPH method for simulating Newtonian and non-Newtonian flows with a free surface. *Advances in water resources*, Vol.26, No.7, 2003, pp. 787-800.
- [11] Nsom, B., Debiante, K., and Piau, J. M., Bed slope effect on the dam break problem. *Journal of Hydraulic Research*, Vol.38, No.6, 2000, pp. 459-464.
- [12] Sun, X., Sakai, M. and Yamada, Y., Three-dimensional simulation of a solid–liquid flow by the DEM–SPH method, *Journal of Computational Physics*, Vol.248, 2013, pp. 147–176.
- [13] Sun, X., and Sakai, M., Three-dimensional simulation of gas–solid–liquid flows using the DEM–VOF method, *Chemical Engineering Science*, Vol.134, 2015, pp. 531-548.
- [14] Gidaspow, D., *Multiphase Flow and Fluidization-Continuum and Kinetic Theory Descriptions*, Academic Press, 1994.